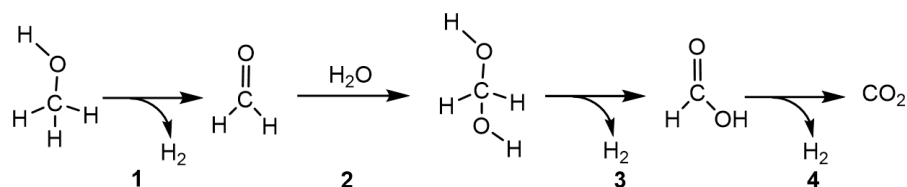


## Summary

### Summary

Development of a new energy infrastructure to combat the climate change and establish a sustainable energy economy is an urgent necessity. This is a broad multidisciplinary problem involving power generation, distribution, and storage. At a fundamental level the solution is rooted in the molecular formulation of energy vectors. For example, hydrogen is a clean burning fuel molecule with high gravimetric energy density but is difficult to produce, distribute and store in a sustainable manner for practical applications. However, using liquid organic molecules such as methanol as carriers of hydrogen presents a viable solution to reversibly store hydrogen equivalents in a stable form in compatibility with present energy infrastructure. Such hydrogen storage systems are called liquid organic hydrogen carriers (LOHC).

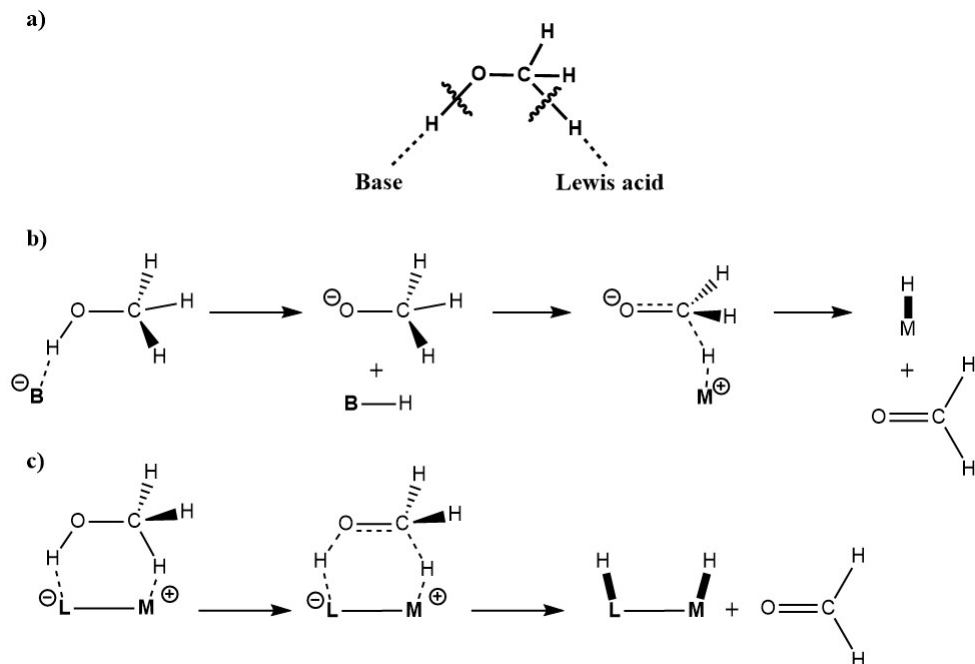
To develop a hydrogen based energy economy using LOHCs, systems/devices capable of producing power from stored hydrogen equivalents in the LOHCs on-demand are needed. Aqueous methanol is an example of an LOHC system, which can store three equivalents of hydrogen. Methanol is a stable liquid under ambient conditions of temperature and pressure, and therefore it requires a rather high activation energy barrier to produce hydrogen from methanol. To reduce this energy barrier, catalytic systems capable of efficiently producing hydrogen equivalents from aqueous methanol are required. This thesis focusses on the elucidating the mechanism of homogeneously catalysed dehydrogenation of aqueous methanol. Dehydrogenation of aqueous methanol to  $\text{CO}_2$  and hydrogen occurs in four steps, which includes formation of formaldehyde, methanediol, formic acid, and finally  $\text{CO}_2$  with stepwise release of three equivalents of hydrogen (see Scheme 1).



*Scheme 1. Four stages (1–4) of the stepwise dehydrogenation of a methanol-water mixture to  $\text{H}_2$  and  $\text{CO}_2$ .*

Computational chemistry methods such as density functional theory (DFT) are used in conjunction with collaborative experimental work to understand the elementary steps involved in dehydrogenation of aqueous methanol by ruthenium (Ru) based catalysts. Dehydrogenation of methanol involves deprotonation of the O-H bond and a C-H activation step necessitating the presence of a base and a Lewis acid acceptor site in the catalytic system (Scheme 2a). Different catalyst design strategies have been developed for this purpose, as described in Chapter 1 of this Thesis. Of those, the metal-ligand cooperative design principle is one of the most advantageous strategies for designing catalysts for aqueous methanol reforming (Scheme 2b and 2c).

## Summary



*Scheme 2. a) General catalyst design strategy for dehydrogenation of methanol to formaldehyde. b) Dehydrogenation of methanol to formaldehyde over a Lewis acidic metal site ( $M$ ) using an external base ( $B$ ) for deprotonation of the  $\text{OH}$  group. c) Metal-ligand cooperative design strategy for dehydrogenation of methanol to formaldehyde over a metal complex with a ligand acting as an internal acceptor base.*

Several catalysts are reported in the literature for aqueous methanol reforming reaction. A truly metal-ligand cooperative catalyst for aqueous methanol reforming should not require presence of additives (base/Lewis acid) for catalytic activity. However, to date the  $[\text{Ru}(\text{trop}_2\text{dad})]$  catalyst reported by the Grützmacher's group is the only catalyst which can perform aqueous methanol reforming under neutral conditions without any additives (base/Lewis acid). Most of the research in this thesis is dedicated to understanding the reactivity and catalysis by this  $[\text{Ru}(\text{trop}_2\text{dad})]$  complex.

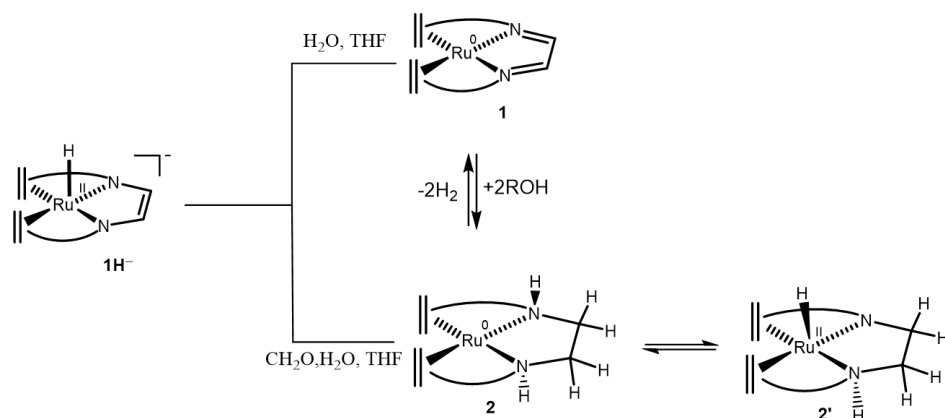
Theoretical concepts and computational methods in computational chemistry are discussed briefly in Chapter 2. To understand chemical reactions at an electronic level of detail one needs to use principles of quantum chemistry, which essentially entails solving the Schrödinger equation. Several approximate methods with varying levels of accuracy are used to solve the Schrödinger equation.

From a computational perspective, a chemical reaction is essentially a rearrangement of reactant(s) on the potential energy surface (PES) to form the product(s). Therefore, practical applications of computational chemistry to molecular systems involve exploration and characterization of parts of the PES of the molecules under investigation. Such an analysis is

## Summary

rather complex and includes optimization of molecular geometry, Hessian and thermochemical calculations, energy calculations, transition state searches etc.

Chapter 3 describes a ruthenium (Ru) based homogeneous catalytic system to produce hydrogen and CO<sub>2</sub> from aqueous formaldehyde. Formaldehyde is an interesting LOHC (a 1:1 formaldehyde/water mixture contains 8.3 wt% of hydrogen). Moreover, the release of dihydrogen from aqueous formaldehyde ( $\text{H}_2\text{CO} + \text{H}_2\text{O} \rightleftharpoons \text{CO}_2 + 2\text{H}_2$ ) is strongly exothermic ( $\Delta H_r = -35.8 \text{ kJ mol}^{-1}$ ), which provides a strong driving force for the production of H<sub>2</sub>. Aqueous formaldehyde is largely present in the form of methanediol, which is formed upon condensation of a formaldehyde molecule with a molecule of water (Scheme 1, stage 2). Experiments showed that the anionic ruthenium hydride precursor complex forms the neutral [Ru(trop<sub>2</sub>dad)] (complex **1**) and [Ru(trop<sub>2</sub>dae)] (complex **2**) complexes under catalytic conditions (Scheme 3).

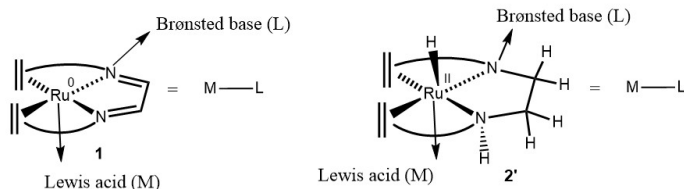


*Scheme 3. Formation of [Ru(trop<sub>2</sub>dad)] and [Ru(trop<sub>2</sub>dae)] complexes from the anionic Ru hydride precursor complex.*

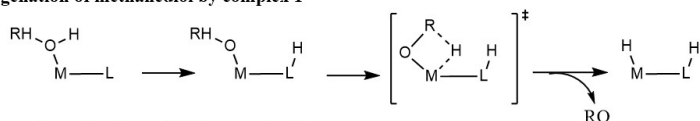
Experiments and DFT calculations consistently showed that both of these complexes are active catalysts for dehydrogenation of methanediol. Dehydrogenation of methanediol to CO<sub>2</sub> and two equivalents of hydrogen proceeds via formation of formic acid as an intermediate (Scheme 1, stages 2-4). DFT calculations showed that the complex **2** with a Ru<sup>0</sup> center first converts to complex **2'** with a Ru<sup>II</sup> center, which is the active catalyst in dehydrogenation of methanediol. In both systems the metal (Ru) and the ligand (N<sub>dad</sub>/N<sub>dae</sub>) cooperate to dehydrogenate the substrate (methanediol/formic acid) and produce hydrogen. The important steps in the mechanism of dehydrogenation of methanediol by complex **1** and **2'** are outlined in Scheme 4.

## Summary

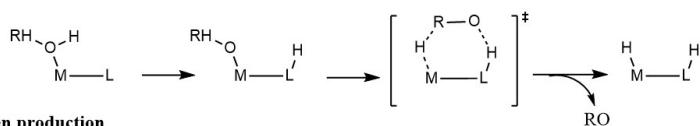
### a) Respective Lewis acid and Brønsted base sites in complexes **1** and **2'**



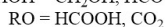
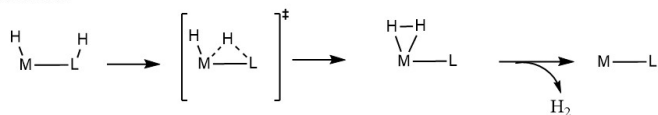
### b) Dehydrogenation of methanediol by complex **1**



### c) Dehydrogenation of methanediol by complex **2'**



### d) Hydrogen production



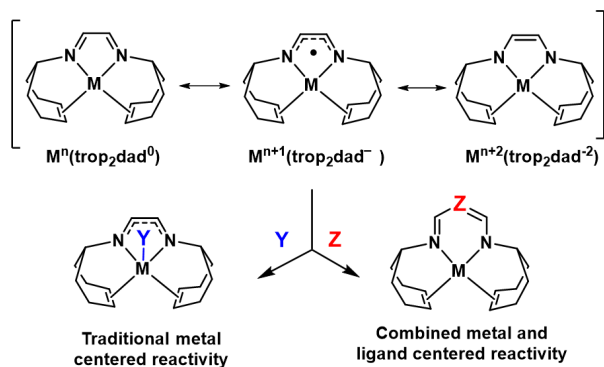
*Scheme 4. a) Respective Lewis acid and Brønsted base sites in complex **1** and complex **2'** that cooperate to dehydrogenate the substrate. b) Dehydrogenation of methanediol/formic acid over complex **1**. While the deprotonation of the  $\text{O-H}$  moiety occurs via a metal-ligand cooperative pathway, a metal-centered classical  $\beta$ -hydride elimination transition state leads to the  $\text{C-H}$  activation step. c) Dehydrogenation of methanediol/formic acid over complex **2'**. The deprotonation of the  $\text{O-H}$  moiety over complex **2'** follows a similar pathway as in the case of complex **1** but the  $\text{C-H}$  activation step proceeds via a non-classical  $\beta$ -hydride elimination pathway. d) In both complexes **1** and **2'** the metal and the ligand cooperate to produce hydrogen in a similar manner.*

In both the catalyst complexes **1** and **2'**, the metal and the ligand cooperate in dehydrogenation of the substrate. The key mechanistic difference between the two systems arises from the ability of the dae ligand to provide hydrogen bonding interaction to the anionic oxygen moiety (in methoxide/formate). While the  $\text{C-H}$  activation step occurs via a classical metal centered  $\beta$ -hydride elimination pathway in complex **1**, the same step undergoes a non-classical  $\beta$ -hydride elimination in complex **2'** with active involvement the ligand via hydrogen bonding interactions.

Chapter 4 describes the electronic structure and reactivity of the  $[\text{Ru}(\text{trop}_2\text{dad})]$  complex. The coordination of diazadiene diolefin ligand to the Ru center forms various complexes of the form  $[\text{Ru}(\text{trop}_2\text{dad})\text{L}]$ . The redox and chemical non-innocence of the dad ligand makes the description of the electronic structure complicated. The electronic structure of the

## Summary

[Ru(trop<sub>2</sub>dad)] complex can be described as Ru<sup>II</sup> with dianionic (bis amido form) dad<sup>2-</sup> ligand, or Ru<sup>0</sup> coordinated to a neutral (bis imine form) of the dad<sup>0</sup> ligand, or a Ru<sup>I</sup> radical coupled to a mono-anionic dad<sup>•-</sup> ligand radical (Scheme 5).



*Scheme 5: Possible valence isomers of a non-innocent dad-diolefin metal complex, giving rise to both metal and ligand centered reactivity.*

DFT studies on the [Ru(trop<sub>2</sub>dad)L] complexes indicate that the closed-shell singlet (CSS), open-shell singlet (OSS) and triplet electronic structures are close in energy indicating a possible multi-reference character of the wavefunction. To assess the multi-reference character, CASSCF calculations were performed on the DFT optimized CSS, OSS and triplet geometries. Consistent with experimental data, the triplet spin state was found to be very high in energy. Singlet state CASSCF calculations showed that the ground state wavefunction possessed a significant multi-reference character in these complexes. While the closed-shell singlet wavefunction dominates, a rather significant (~8-16%) open-shell singlet [d<sup>7</sup>-Ru(I)(L)(trop<sub>2</sub>dad<sup>•-</sup>)] contribution is mixed into the ground state. In agreement with their ambivalent electronic structure, these complexes reveal both metal and ligand centered reactivity. B3LYPXC functional DFT calculations were performed to study the mechanism of scission of C—C<sub>trop</sub> bond upon reaction with AdN<sub>3</sub> and diazomethane species. These calculations showed that the metal and ligand cooperate in these reactions and the radical character of the dad<sup>•-</sup> ligand helped lowering the reaction barrier via OSS and triplet pathways.

Chapter 5 provides a detailed DFT study on the mechanism of complete dehydrogenation of aqueous methanol by the [Ru(trop<sub>2</sub>dad)] complex. Analysis of the DFT optimized geometry, and the potential energy surface of the methanol adduct of [Ru(trop<sub>2</sub>dad)] revealed a significant contribution of the Ru<sup>0</sup> coordinated to a neutral (bis imine) dad<sup>0</sup> ligand to the electronic structure of the metal complex.

## Summary

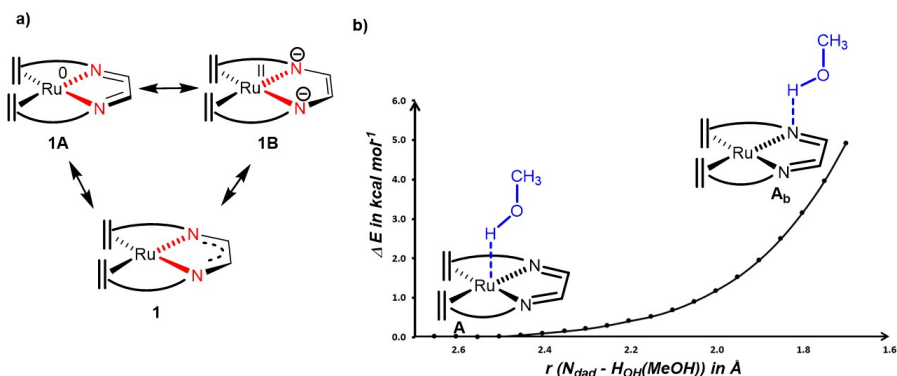


Figure 1. a) The electronic structure of complex **1** is best described by two contributing resonance structures: **1A** with ruthenium in oxidation state 0 coordinated to a neutral dad moiety and **1B** with ruthenium in oxidation state +II coordinated to a dianionic dad moiety. b) Potential energy surface (PES) scan to drive the  $H_{OH}$  in methanol ( $H_{OH}(MeOH)$ ) to one of the  $N_{dad}$  atoms. In complex **A**, methanol prefers to bind via the OH group to the metal center indicating a larger contribution of resonance structure **1A** to the ground state of complex **1**. The vertical axis represents the relative SCF energy ( $\Delta E$ ) (BP86/def2-SVP) while the horizontal axis represents the distance between the  $N_{dad}$  atom and MeOH hydroxyl proton.

DFT calculations revealed  $\pi$ -coordination of the dad ligand to the Ru center as an energetically feasible process. Further analysis of the frontier orbitals and natural charges revealed that the  $\pi$ -coordination process enhanced the Lewis acidity and Brønsted basicity of the Ru and  $N_{dad}$  centers respectively (Figure 2).

## Summary

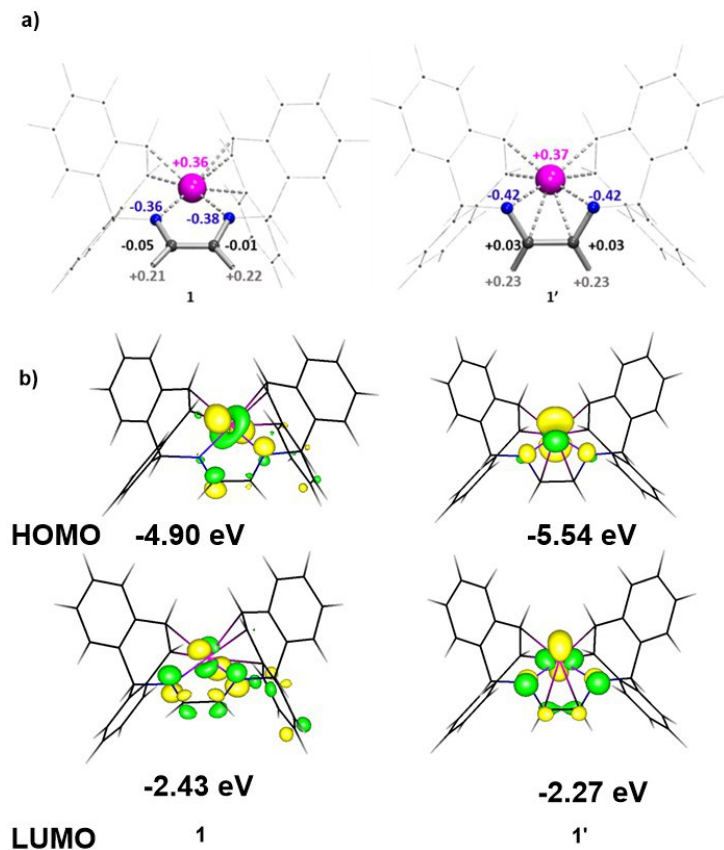


Figure 2. a) Natural population analysis of complexes **1** and **1'**. The most relevant parts of the complexes are highlighted for clarity. b) Frontier orbitals (HOMO-LUMO) of complexes **1** and **1'**. (BP86//B3LYP (Water))

Dehydrogenation of a substrate molecule (methanol/methanediol/formic acid) was found to proceed via a metal-ligand cooperative Noyori-Morris-type mechanism which included deprotonation of the O–H moiety and the C–H activation steps simultaneously over the N<sub>dad</sub> and Ru centers respectively resulting in hydrogenation of the Ru–N<sub>dad</sub> bond. Cooperation of metal and the N<sub>dad</sub> ligand leads to hydrogen production. The computed transition states with relevant bond lengths are shown in Figure 3.

## Summary

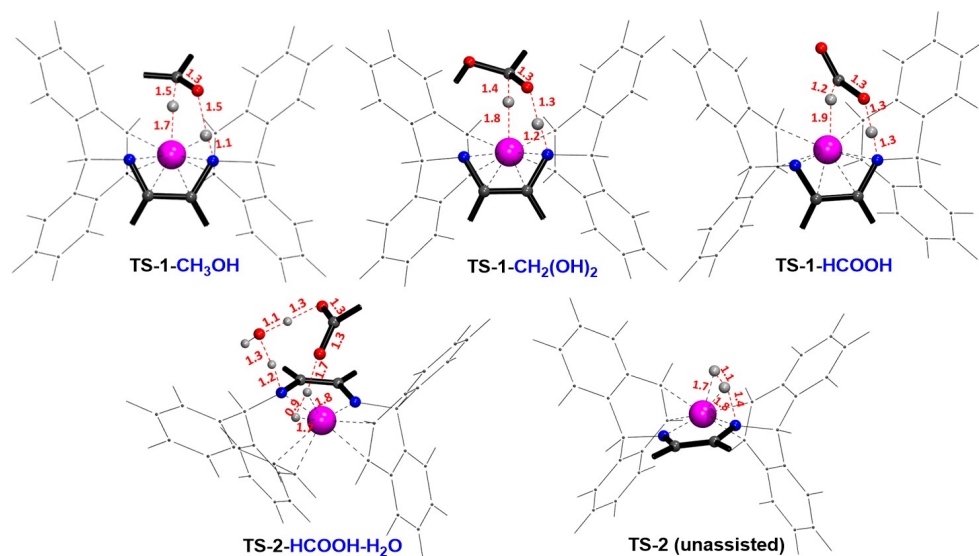


Figure 3. Snapshots of optimized geometries of the transition states reported in the main text along relevant bond lengths (in Å).

A comparison of reaction pathways with and without  $\pi$ -coordination reveals that  $\pi$ -coordination significantly lowers the transition state barriers and provides a more favourable, lower energy reaction pathway on the potential energy surface for dehydrogenation of aqueous methanol. In light of the new discovered  $\pi$ -coordination transformation, the mechanism for dehydrogenation of methanediol to CO<sub>2</sub> and two equivalents of H<sub>2</sub> over the [Ru(trop<sub>2</sub>dad)] complex (as discussed in chapter 3) is revised in this chapter. We also investigated complex 2' (see Scheme 4a) as a catalyst for dehydrogenation of aqueous methanol. For this system it was found that the explicit solvent molecules form an integral part of the reactive system, and solvent effects are crucial in the modelling of the dehydrogenation reaction.

Chapter 6 provides a case study of solvent effects in methanol dehydrogenation over the Ru(PNP) complex. DFT based molecular dynamics (DFT-MD) calculations on the Ru(PNP) system in a box of explicit solvent molecules revealed that the N<sub>PNP</sub> moiety is strongly basic and unlikely to get deprotonated by external base present under the experimentally applied catalytic reaction conditions (Figure 4). On the basis of (computationally expensive) DFT-MD calculations with fully explicit solvent molecules, micro-solvated static DFT models were developed to model the reaction pathways with including the solvent effects at a modest computational expense.

## Summary

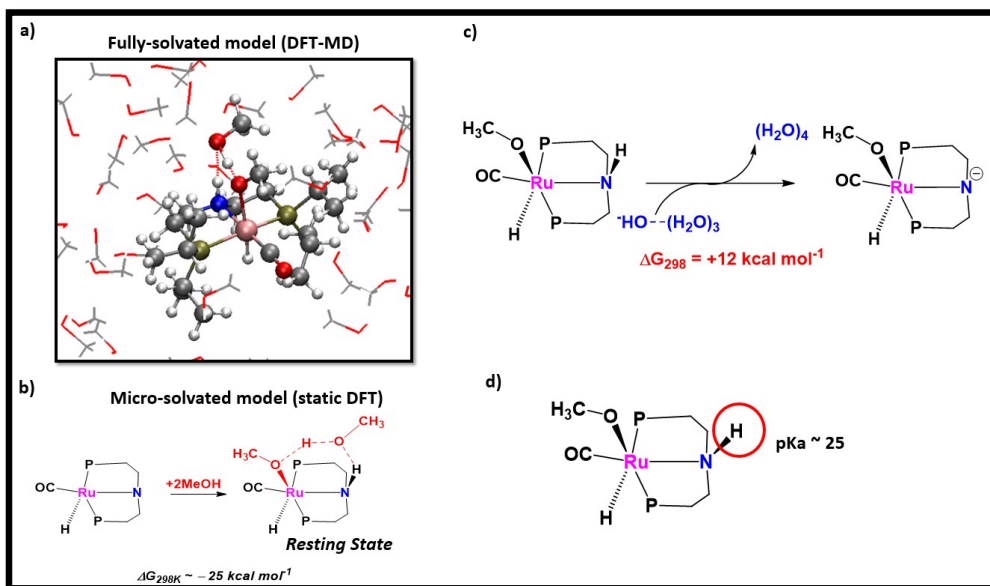


Figure 4. (a) Methanol adduct of the Ru(PNP) system in a solvent box. (b) Micro-solvated static DFT model based on DFT-MD simulations. A methoxide adduct with protonated amido moiety was found to be the resting state. (c) Deprotonation of amine moiety to generate the anionic methoxide adduct by a micro-solvated hydroxide moiety was found to be endergonic by 12 kcal mol<sup>-1</sup> demonstrating the strong basicity of the N<sub>PNP</sub> amido function. (d) pK<sub>a</sub> of the N-H function with a methoxide moiety coordinated to the metal center was estimated to be about 25, indicating that it would be energetically challenging to deprotonate it even with 8M KOH present during the catalytic conditions.

These calculations revealed a new metal-centered pathway for dehydrogenation of methanol. During the entire catalytic cycle, the amido moiety stays protonated (Scheme 6). Deprotonation of methanol to generate the methoxide moiety occurred with hence requires the help of external inorganic base, which acts as a promoter. Stabilization of the resulting methoxide anion by hydrogen bonding with explicit solvent molecules increases the energy barrier for the C-H activation step compared to a system where such interactions are absent (Figure 5). The C-H activation results in transfer of a hydride to the metal center to generate the hydrogenated metal complex.



## Summary

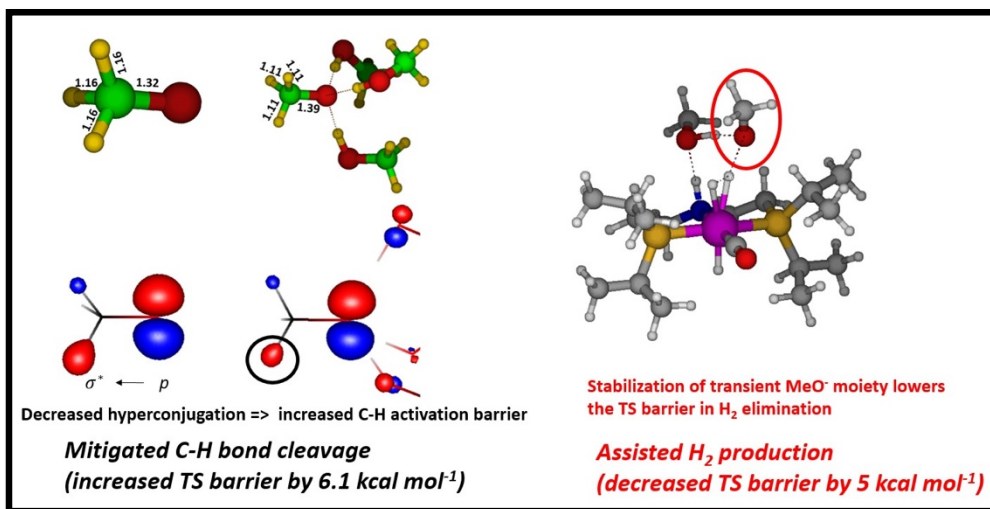


Figure 5. Left: Bond lengths (top) and HOMO (bottom) of a bare methoxide anion versus a solvated methoxide anion hydrogen bonded to three methanol molecules. The C–H bond length decreases upon solvation due to decreased hyperconjugation effect. The orbital lobe on the hydride moiety shrinks upon solvation which further attests to a decrease in hyperconjugation. Right: TS geometry during solvent assisted hydrogen production in the Ru(PNP) system. The transient methoxide moiety that is generated upon protonation of the Ru–H bond is favorably stabilized by the extra solvent molecule which lowers the TS barrier for hydrogen production.

The computational study performed in this chapter provides new insight on methanol dehydrogenation and metal-ligand cooperativity in the presence of a protic hydrogen bonding solvent environment.

## Outlook

Several new projects based on the research conducted as part of this PhD thesis can be envisioned. The [Ru(trop<sub>2</sub>dad)] system is to date the only catalytic system that can perform dehydrogenation of aqueous methanol under neutral conditions without any additives (Lewis acid/base). The peculiar metal-ligand cooperativity resulting from  $\pi$ -coordination provide a direction to look for highly efficient catalysts for methanol dehydrogenation that can operate under neutral conditions and in an additive free manner. Therefore, a further research direction could be to look for other metal-ligand combinations where metal-ligand cooperativity can be harnessed in a similar manner.

A comparison of the contrasting mechanisms of the [Ru(trop<sub>2</sub>dad)] and the Ru(PNP) systems for methanol dehydrogenation stress on the importance of the  $pK_a$  of the ligand when designing metal-ligand cooperative systems for methanol dehydrogenation. This observation is summarized in Figure 6

## Summary

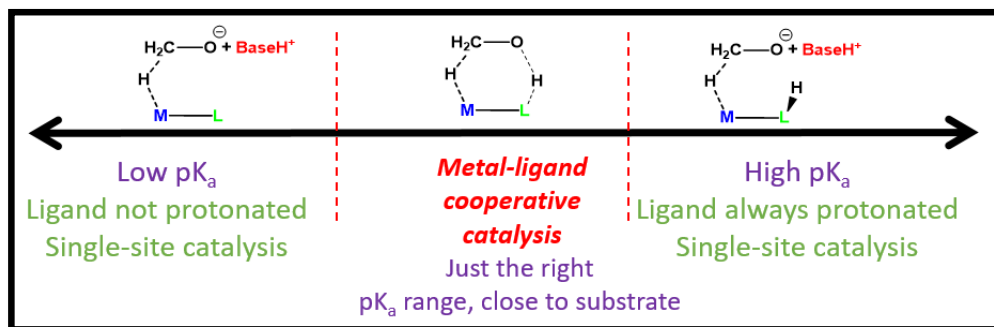


Figure 6. Effect of the  $pK_a$  of the ligand in designing a metal-ligand cooperative additive free catalytic system for dehydrogenation of methanol.

If the  $pK_a$  of the protonated ligand is very low it will cost a lot of energy to protonate it, and an external base will be required to deprotonate methanol before C–H activation can occur. For a system with a highly basic ligand (high  $pK_a$  upon protonation), once the ligand is protonated it will be difficult to deprotonate it again, making it unavailable for deprotonating methanol in the catalytic cycle. In this case again an external base will be required for catalysis. However, if the  $pK_a$  of the protonated ligand is close to that of the solvent/methanol, it will be easier to protonate/deprotonate it reversibly during the catalytic cycle, and an external base will therefore not be needed. This observation can be used to screen ligands for design of base free metal-ligand cooperative catalysts for methanol dehydrogenation. A further research direction could be to perform  $pK_a$  calculations on catalysts known for methanol dehydrogenation in the literature, and then computationally perform various ligand modifications to come up with functional strategies to fine-tune the  $pK_a$  of the protonated ligand. A similar strategy can be used to explore methods to tune the Lewis acidity of the metal center as well to discover novel catalytic systems.

The importance of modelling reaction pathways with explicit solvent molecules is stressed by the mechanistic studies of methanol dehydrogenation over complex **2'** and the Ru(PNP) system. Specifically, the development of micro-solvated static DFT models to accurately capture solvent effects at a lower computational cost (than DFT-MD calculations)(chapter 6) sets a research direction for future mechanistic investigations of catalytic systems involving protic solvent environments.